University of Wollongong
Research Online

Australian Institute for Innovative Materials - Papers

Australian Institute for Innovative Materials

2006

Thermionic cooling in cylindrical semiconductor nanostructures

Pin Lyu
University of Wollongong

Chao Zhang
University of Wollongong, czhang@uow.edu.au

Publication Details

Lyu, P & Zhang, C (2006), Thermionic cooling in cylindrical semiconductor nanostructures, Applied Physics Letters, 89(15), pp. 153125-1-153125-3.

Research Online is the open access institutional repository for the University of Wollongong. For further information contact the UOW Library: research-pubs@uow.edu.au

Thermionic cooling in cylindrical semiconductor nanostructures

Abstract
The authors analyzed the thermionic cooling efficiency of the cylindrical semiconductor nanostructures. It is shown that due to the reduced emission current from the inner electrode, the cooling efficiency can be enhanced if the outer cylinder is the cold electrode. The threshold voltage for thermionic cooling is lower in cylindrical devices as compared to that in planar devices. The competition between the heat transport by electrons and the heat conduction by phonons is responsible for the efficiency enhancement and the voltage reduction.

Keywords
Thermionic, cooling, cylindrical, semiconductor, nanostructures

Disciplines
Engineering | Physical Sciences and Mathematics

Publication Details
Lyu, P & Zhang, C (2006), Thermionic cooling in cylindrical semiconductor nanostructures, Applied Physics Letters, 89(15), pp. 153125-1-153125-3.

This journal article is available at Research Online: http://ro.uow.edu.au/aiimpapers/72

Thermionic cooling in cylindrical semiconductor nanostructures

Pin Lyu and Chao Zhang[a)]
School of Engineering Physics, University of Wollongong, New South Wales 2522, Australia

(Received 20 July 2006; accepted 28 August 2006; published online 12 October 2006)

The authors analyzed the thermionic cooling efficiency of the cylindrical semiconductor nanostructures. It is shown that due to the reduced emission current from the inner electrode, the cooling efficiency can be enhanced if the outer cylinder is the cold electrode. The threshold voltage for thermionic cooling is lower in cylindrical devices as compared to that in planar devices. The competition between the heat transport by electrons and the heat conduction by phonons is responsible for the efficiency enhancement and the voltage reduction. © *2006 American Institute of Physics*. [DOI: 10.1063/1.2361263]

The basic structure of the thermionic cooler consists of two planar electrodes separated by a potential barrier, such as metal-vacuum-metal system.[1] Recently, thermionic devices based on semiconductor layered structures (e.g., doped quantum wells separated by undoped barriers) were proposed and investigated.[2,3] The semiconductor systems were considered as a promising candidate for thermionic cooling due to their low work functions. The science of thermionics and its potential application in integrated cooling of electronic and optoelectronic devices have attracted considerable interest both theoretically and experimentally.

Several schemes have been proposed to improve the cooling efficiency, including multilayer structures,[3] optothermionic refrigeration,[4] nonconserved lateral momentum,[5] injected electrons via resonant tunneling,[6] reversible electronic transport,[7] and zigzagged barrier.[8] In experiments, the cooling of up to a few degrees was reported in thermionic cooling devices.[9–11] It is still a challenge to search for different mechanisms and structures for high efficiency of thermionic cooling.

Most thermionic cooling devices are based on the planar semiconductor nanostructures. In such a thermionic cooler, the applied voltage must exceed threshold voltages above which both the electrical and heat currents are flowing from the cold electrode to the hot electrode. This threshold voltage represents the minimum bias for the current to flow again the temperature gradient. To lower the threshold voltage, one needs to enhance the emission of the cold electrode relative to that of the hot electrode or to reduce the thermal conductivity due to phonons. In this letter, we propose to use cylindrical semiconductor nanostructures for thermionic cooling. In such structures, the emission from the inner electrode is always smaller than that from the outer electrode. As a result, a lower threshold voltage and higher efficiency can be achieved.

Figure 1 shows the schematics of the cylindrical semiconductor nanostructures with the outer cylinder as the cold electrode. According to Richardson's formalism, the thermionic electrical current densities emitted from the inner and outer electrodes are given by

$$J_E^{a(b)} = e \int \mathbf{v_k} \cdot \mathbf{n} f(E_k - E_F^{h(c)}, T_{h(c)}) g(k) d\mathbf{k}, \tag{1}$$

with the integrals limited in the ranges of $E_{k_r} - E_F^h > U_0 + eV$ and $E_{k_r} - E_F^c > U_0$, respectively. Here U_0 is the work function of the electrode, $\mathbf{n}$ is the radial unit vector, $k_r = \mathbf{k} \cdot \mathbf{n}$, the density of states $g(k) = 2/(2\pi)^3$, $f(E_k - E_F, T)$ is the Fermi-Dirac distribution function, $E_k = \hbar^2 k^2 / 2m^*$, $\mathbf{v_k} = (1/\hbar)\nabla E_k$, and T_h and T_c are the temperatures of the hot and cold electrodes. The electron charge e is taken as positive for clearness.[3]

The total net electrical current density $J_E(r)$ at any position inside the barrier region satisfies the total current conservation, $2\pi a L J_E^a + 2\pi b L J_E^b = 2\pi r L J_E(r)$, where L is the length along the z direction and $2\pi r L$ is the area normal to the direction of electronic transport. We obtain

$$J_E(r) = \frac{a J_E^a + b J_E^b}{r}, \tag{2}$$

where r is in the range of $a \leqslant r \leqslant b$. From the above equation, the net electrical current density at the outer electrode is obtained as $J_E(b) = (a/b) J_E^a + J_E^b$, which is dependent on the radii a and b of the cylinder.

The heat current densities accompanied with the emitted electrical current densities from the hot and cold electrodes are given by

$$J_Q^{a(b)} = \int (E_k - E_F^c) \mathbf{v_k} \cdot \mathbf{n} f(E_k - E_F^{h(c)}, T_{h(c)}) g(k) d\mathbf{k}, \tag{3}$$

with the integrals limited in the same ranges as that for the Eq. (1).

Across the barrier, there exists the heat conduction by phonons. The corresponding heat transfer density from the hot electrode to the cold electrodes in a cylinder structure is given as[12] $q''(r) = \kappa \Delta T / [r \ln(b/a)]$, where $\Delta T = T_h - T_c$ and κ is the thermal conductivity of the barrier materials. To get this result, one needs to find the temperature distribution by solving the heat equation with the cylindrical boundary condition. After the temperature distribution is obtained, the heat transfer density is given by Fourier's law $q'' = -\kappa \nabla T$.

The total net heat transfer density $J_Q(r)$ at any position r $(a \leqslant r \leqslant b)$ satisfies the energy balance equation, $2\pi a L J_Q^a + 2\pi b L J_Q^b + 2\pi r L q''(r) = 2\pi r L J_Q(r)$. Then we get

[a)]Electronic mail: czhang@uow.edu.au

 © 2006 American Institute of Physics

Downloaded 08 Oct 2012 to 130.130.37.84. Redistribution subject to AIP license or copyright; see http://apl.aip.org/about/rights_and_permissions

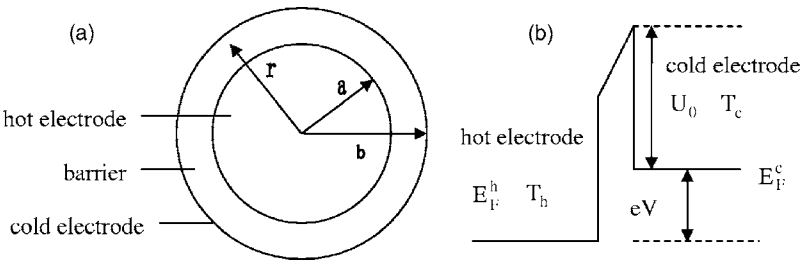

FIG. 1. Schematics for thermionic cooling in cylindrical semiconductor nanostructures with the outer cylinder as the cold electrode.

$$J_Q(r) = \frac{aJ_Q^a + bJ_Q^b}{r} + \frac{\kappa\Delta T}{r\ln(b/a)}. \quad (4)$$

At the cold electrode, the net heat density can be written as $J_Q(b)=(a/b)J_Q^a+\kappa\Delta T/b\ln(b/a)+J_Q^b$.

The cooling efficiency is defined as $\eta^R = J_Q(b)/[J_E(b)V]$. For the present system, we obtain

$$\eta^R = \frac{(a/b)J_Q^a + \kappa\Delta T/b\ln(b/a) + J_Q^b}{((a/b)J_E^a + J_E^b)V}. \quad (5)$$

The efficiency is now determined by the radii a and b. Let us discuss the limit situations. For $a \gg d$, where $d \equiv b-a$ is the barrier width, the resulting cooling efficiency η^R in Eq. (5) is reduced to the formula of the conventional layer structure with two parallel plate electrodes as follows: $\eta^R=(J_Q^a+\kappa\Delta T/d+J_Q^b)/[(J_E^a+J_E^b)V]$. In the limit of small cylinders, we have $\eta^R=J_Q^b/(J_E^bV)$ from Eq. (5), where we had used $\kappa\Delta T/b\ln(b/a)\to 0$ with $a\to 0$. At this limit, the heat conduction is frozen and the heat load disappears.

As a requirement for thermionic emission, the electron must be thermally excited over the barrier and no tunneling through the barrier occurs. The barrier width d for most semiconductors is between 10 and 100 nm.[3] Further to satisfy the continuing energy spectrum for thermal electron emission used in the present formalism, the radius of the inner cylinder should be more than the nanometer size, $a \geqslant 100$ nm. In numerical calculation, we used parameters of GaAs/AlGaAs/GaAs structures, $m^*=0.07m_e$, $E_F^h=15$ meV, $U_0=0.1$ eV, and the lattice thermal conductivity $\kappa=5$ W/mK, estimated from the experiment.[13] The working temperatures are $T_c=620$ K and $T_h=650$ K.

In Fig. 2 we show the cooling efficiency of cylindrical structures with the outer cylinder as the cold electrode. The cooling characteristics vary with the inner radius a and the barrier width d. At fixed a (Fig. [2(a)], the enhancement of η with d is mainly due to the reduction of phonon heat current. This d dependence is common to both planar and cylindrical structures. Figure 2(b) shows the enhancement of η and the reduction of threshold voltage as a decreases while d is fixed. It can be seen that better performance can be achieved with smaller cylinders. Figure 3 illustrates the threshold voltage for different inner radius a. For a fixed barrier width, for example, $d=70$ nm, the threshold voltage increases with the radius of the inner cylinder and finally reaches the value of two planar structures at very large radius a. For special parameter $d=50$ nm, the threshold voltage of the planar system is not defined. By the combination of Figs. 2(b) and 3, we notice that the cylinder structures may work well under small voltages below the threshold voltage of the corresponding planar structures. This situation is shown in Fig. 2(b) for voltages between 0.025 and 0.050 V. A cooling efficiency higher than 0.8 can be achieved.

Figure 4 shows the cooling efficiency versus the radius of the inner cylinder at several fixed barrier widths. The applied voltage is kept at $V=0.08$ V. The cooling efficiency increases with the decreasing radius of the inner cylinder. This is because (i) the heat backflow due to phonons decreases with a, and (ii) the ratio of the total thermionic emission from the cold electrode to that from the hot electrode increases with a. For narrow barriers, there exists a cutoff radius a_c above which cooling cannot be achieved. If the barrier is wide enough such that a_c does not exist, the effi-

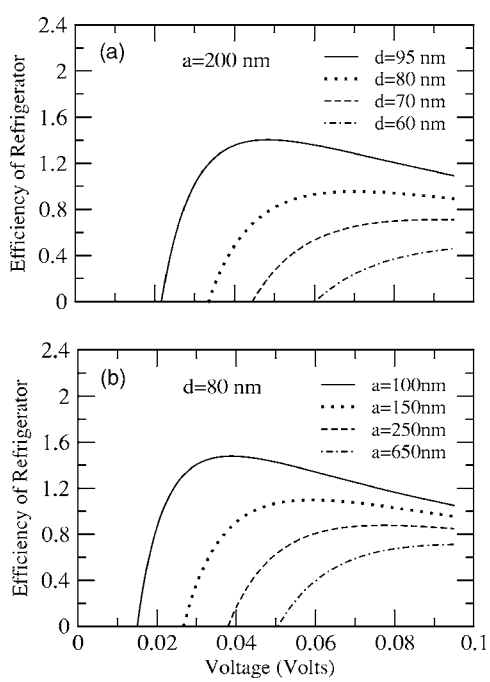

FIG. 2. Cooling efficiency of cylindrical structures (with the outer cylinder as the cold electrode) vs the applying voltage at a fixed radius of the inner cylinder (a) and at a fixed width of barrier (b).

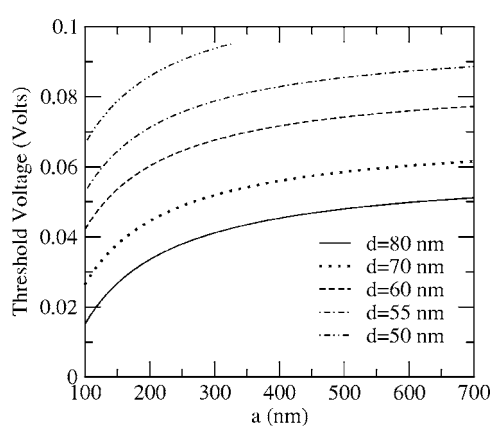

FIG. 3. Threshold voltage vs the radius of the inner cylinder at several fixed widths of the barrier.

Downloaded 08 Oct 2012 to 130.130.37.84. Redistribution subject to AIP license or copyright; see http://apl.aip.org/about/rights_and_permissions

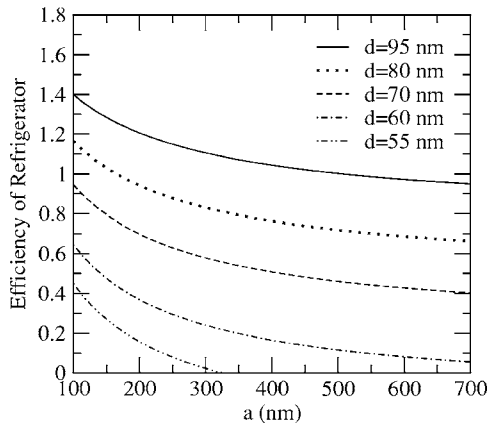

FIG. 4. Cooling efficiency of cylindrical structures (with the outer cylinder as the cold electrode) vs the radius of the inner cylinder at several fixed barrier widths.

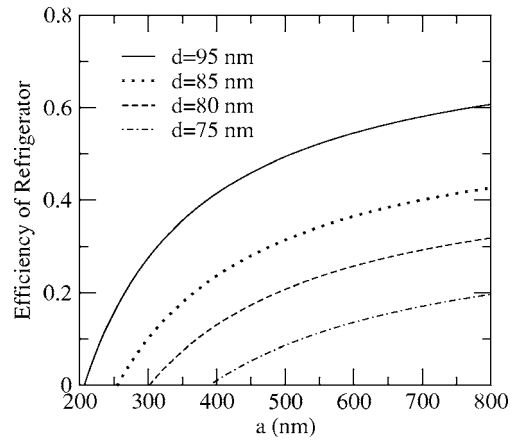

FIG. 5. Cooling efficiency of cylindrical structures (with the outer cylinder as the hot electrode) vs the radius of the inner cylinder at several fixed barrier widths.

ciency approaches the corresponding values of the planar structure. Thus we may achieve higher cooling efficiency by using smaller cylindrical structures with a fixed barrier width.

Unlike the planar structure, there is no symmetry in exchanging the hot and cold electrodes in the cylinder structure. Using the inner cylinder as a cold electrode is not beneficial to the thermionic cooling with the maximum cooling efficiency no more than that of the two parallel plates. When the radius of the inner cylinder is very large compared with the barrier width, the cooling efficiency approaches the corresponding values of two parallel plates. Figure 5 shows this behavior, where the parameters are the same as those used in Fig. 4. There exists the threshold radius a_t of the inner cylinder for different barrier widths, for example, $a_t = 302$ nm for $d = 80$ nm. The refrigerator with $a > a_t$ and a suitable barrier width begin to work. It should be emphasized that the thermionic cooling efficiency is enhanced by using the outer cylinder as the colde electrode while it is suppressed with the inner cylinder as a cold electrode. The improvement in efficiency presented here is purely due to the change from planar to cylindrical geometry. Any previous improving strategies[3–8] can be applied to further enhance the cooling efficiency in this structure.

We emphasize that results given in Figs. 3–5 show some advantage of using cylindrical structures and devices perform better as a decreases at fixed d. The d dependence of η is common to both planar and cylindrical structures therefore does not represent the advantage of the cylindrical structure. The reason of plotting the same a-dependence curve with several different d is not to show the enhancement of η with d but rather to demonstrate that the a dependence is not altered when d varies.

In summary, we have shown that thermionic cooling efficiency can be improved with the use of cylindrical semiconductor structures. Such systems also have smaller threshold voltages. The competition between the heat transport by electrons and the heat conduction by phonons is responsible for the efficiency enhancement and the voltage reduction.

This work was supported by the Australia Research Council.

[1] G. D. Mahan, J. Appl. Phys. **76**, 4362 (1994).
[2] A. Shakouri and J. E. Bowers, Appl. Phys. Lett. **71**, 1234 (1997).
[3] G. D. Mahan and L. M. Woods, Phys. Rev. Lett. **80**, 4016 (1998); G. D. Mahan, J. O. Sofo, and M. Bartkowiak, J. Appl. Phys. **83**, 4683 (1998).
[4] A. G. Mal'shukov and K. A. Chao, Phys. Rev. Lett. **86**, 5570 (2001).
[5] D. Vashaee and A. Shakouri, Phys. Rev. Lett. **92**, 106103 (2004).
[6] K. A. Chao, M. Larsson, and A. G. Mal'shukov, Appl. Phys. Lett. **87**, 022103 (2005).
[7] M. F. O'Dwyer, R. A. Lewis, C. Zhang, and T. E. Humphrey, Phys. Rev. B **72**, 205330 (2005).
[8] Z. Bian and A. Shakouri, Appl. Phys. Lett. **88**, 012102 (2006).
[9] A. Shakouri, C. LaBounty, J. Piprek, P. Abraham, and J. E. Bowers, Appl. Phys. Lett. **74**, 88 (1999).
[10] X. Fan, G. Zeng, C. LaBounty, J. E. Bowers, E. Croke, C. C. Ahn, S. Huxtable, A. Majumdar, and A. Shakouri, Appl. Phys. Lett. **78**, 1580 (2001).
[11] Y. Hishinuma, T. H. Geballe, B. Y. Moyzhes, and T. W. Kenny, J. Appl. Phys. **94**, 4690 (2003).
[12] F. P. Incropera and D. P. DeWitt, *Fundamentals of Heat and Mass Transfer*, 5th ed. (Wiley, New York, 2001), p. 564.
[13] W. S. Capinski, H. J. Maris, T. Ruf, M. Cardona, K. Ploog, and D. S. Katzer, Phys. Rev. B **59**, 8105 (1999).

Downloaded 08 Oct 2012 to 130.130.37.84. Redistribution subject to AIP license or copyright; see http://apl.aip.org/about/rights_and_permissions